Gravitational-wave Extraction using Independent Component Analysis

arXiv:2503.14179

Hisaaki Shinkai, Rika Shimomura, Yuuichi Tabe
(Osaka Institute of Tech., Japan)

Motivations

- New method proposal for GW extraction without templates
  - Test of GR
  - Unknown GW

Conclusions

- Injection tests with real data: OK for SNR>15
- Applied for 10+ known events (upto O3)
  - can extract GW, consistent Mc(1+z) with GWTC3
  - more precise arrival time can be derived

GW150914

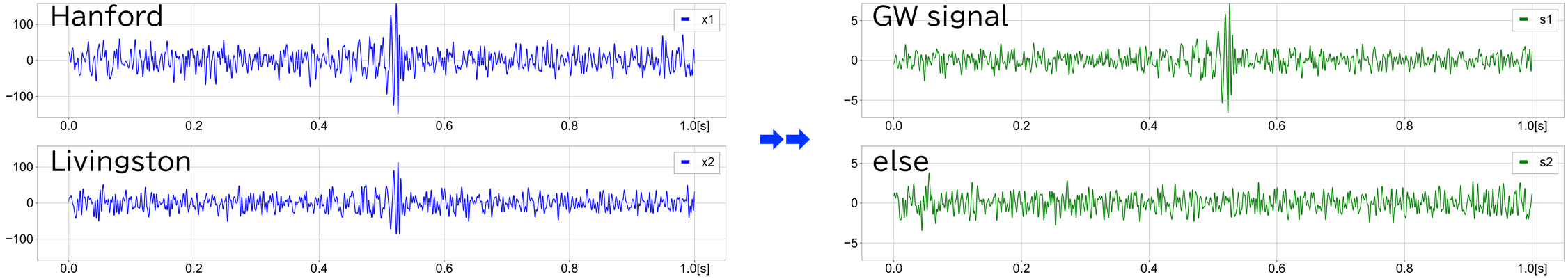

Independent Component Analysis (ICA)

A method for finding hidden factors or components in multivariate data,
where the components to be found are statistically independent and non-Gaussian.

Blind Source Separation

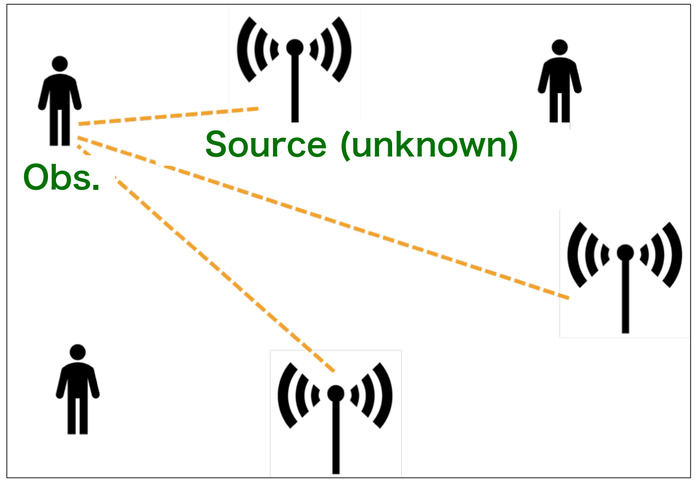

3 observed data from 3 sources

$$\boldsymbol{x}(t) = A\boldsymbol{s}(t)$$

Observed Signals — Combination Matrix — Source Signals

$$\tilde{\boldsymbol{s}}(t) = W\boldsymbol{x}(t)$$

Candidate Source Signals — Observed Signals

Find out this Matrix!

Independent Component Analysis (ICA)

A method for finding hidden factors or components in multivariate data,
where the components to be found are statistically independent and non-Gaussian.

Blind Source Separation

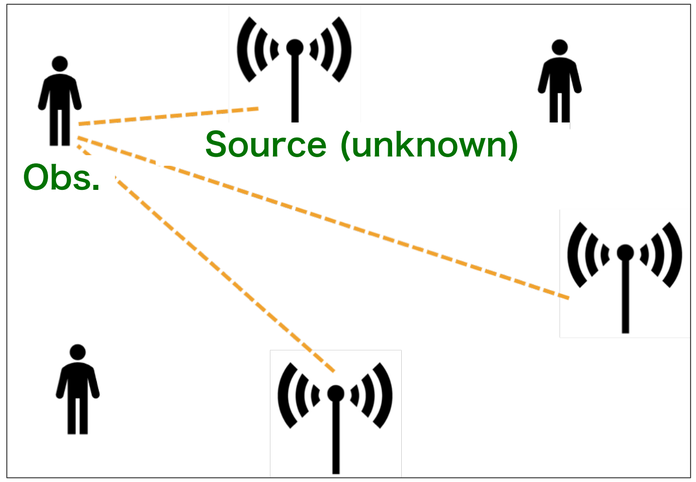

3 observed data from 3 sources

$$\boldsymbol{x}(t) = A\boldsymbol{s}(t)$$

Observed Signals — Combination Matrix — Source Signals

$$\tilde{\boldsymbol{s}}(t) = W\boldsymbol{x}(t)$$

Candidate Source Signals — Observed Signals

Find out this Matrix!

Extract statistically independent non-Gaussian signals

... Search for signals that are far from Gaussian

Whitening data to $z(t)$

$$s_i(t) = \boldsymbol{w}_i^T V \boldsymbol{x}(t) \equiv \boldsymbol{w}_i^T \boldsymbol{z}(t)$$

Find the matrix W which maximizes the kurtosis

$$\mathrm{kurt}(\boldsymbol{w}^T\boldsymbol{z}) = E[(\boldsymbol{w}^T\boldsymbol{z})^4] - 3\{E[(\boldsymbol{w}^T\boldsymbol{z})^2]\}^2$$

using repeated process until converge

$$\frac{\partial}{\partial \boldsymbol{w}_i}|\mathrm{kurt}(\boldsymbol{w}_i^T\boldsymbol{z})| = \begin{pmatrix} E[4(\boldsymbol{w}_i^T\boldsymbol{z})^3\boldsymbol{z}_1] \\ E[4(\boldsymbol{w}_i^T\boldsymbol{z})^3\boldsymbol{z}_2] \\ \vdots \end{pmatrix} - 12||\boldsymbol{w}_i||^2 \begin{pmatrix} w_{11} \\ w_{12} \\ \vdots \end{pmatrix}$$

Practically, kurtosis is sensitive to outliers.
We use g-function method, instead.

$$\boldsymbol{w}_p = E[\boldsymbol{z}g(\boldsymbol{w}_p^T\boldsymbol{z})] - E[g'(\boldsymbol{w}_p^T\boldsymbol{z})]\boldsymbol{w}$$

where $g(y) = \tanh y$. (one of FastICA method)

Application of ICA to GW data analysis : Past proposals

references

[1] R. De Rosa, et al., CQG 29, 215008 (2012)
Proposed to apply ICA for preprocess of matched-filtering analysis. Demonstrate with detector mock-data and GW mock-data.

[2] S. Morisaki, J. Yokoyama, K. Eda, Y. Itoh, J.Comp. Phys. 300, 275 (2016)
Proposed application of non-Gaussian noise deletion

[3] KAGRA Collaboration, CQG 40, 085015 (2023)
Applied ICA to iKAGRA data (2020) together with physical environment data, and show seismic noise reduction

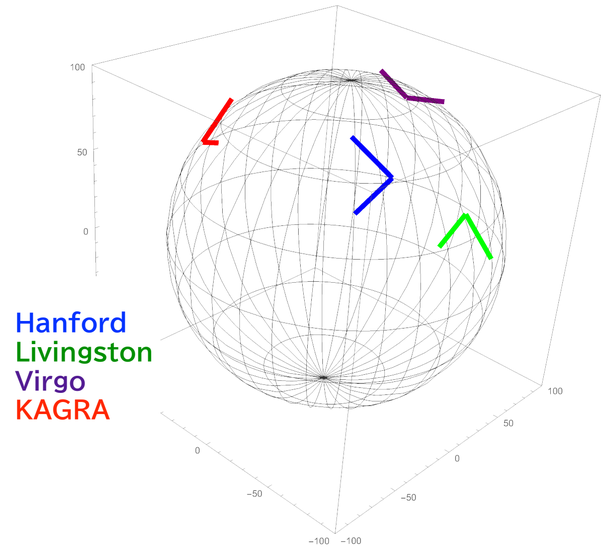

➢No trials yet for GW extraction for real detector data

Need to check

Can we extract GW from real detector data?
How much SNR is required?

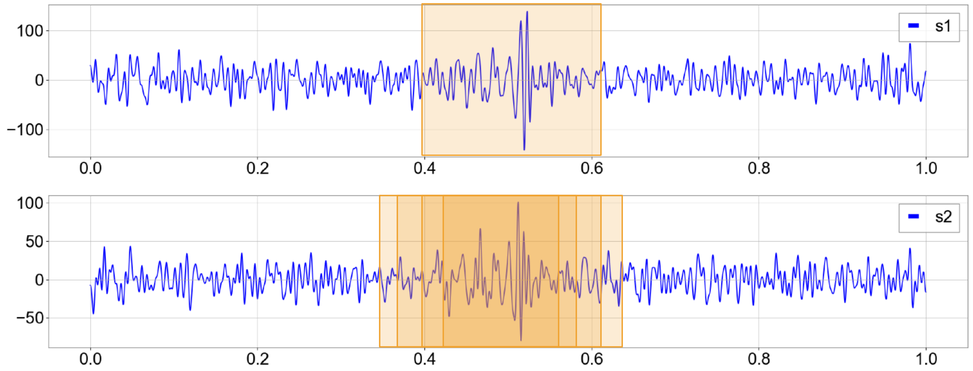

Shift the detector data corresponding to the arrival time

Test 1: 2 different Gaussian noise+inspiral-wave injection

$$\text{Model 1}: \begin{cases} x_1(t) = n_{1\mathrm{G}}(t) + h_{\mathrm{insp}}(t; t_c, M_c), \\ x_2(t) = n_{2\mathrm{G}}(t) + h_{\mathrm{insp}}(t; t_c, M_c). \end{cases}$$

extraction from Gaussian noise is hard for small amplitude signals

injection wave = 5 x noise

input x(t)

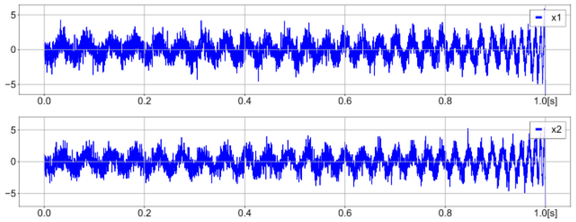

(a1) Input signals with $|h_{\mathrm{insp}}(t=1)|/\overline{|n_{\mathrm{G}}(t)|} = 5.0$.

input x(f)

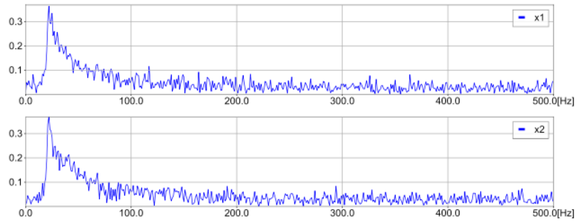

(a2) Fourier spectrum of (a1).

output s(t)

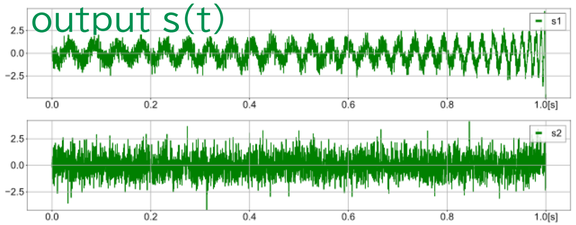

(a3) Output of ICA for (a1).

output s(f)

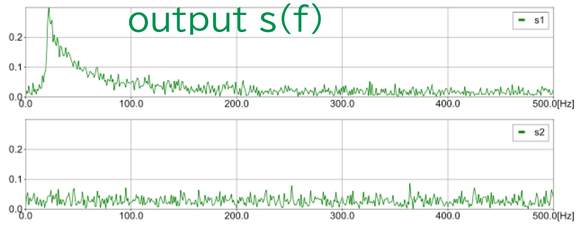

(a4) Fourier spectrum of (a3).

injection wave = 2.5 x noise

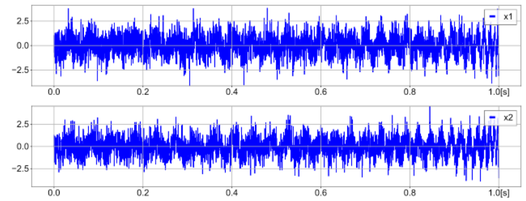

(b1) Input signals with $|h_{\mathrm{insp}}(t=1)|/\overline{|n_{\mathrm{G}}(t)|} = 2.5$.

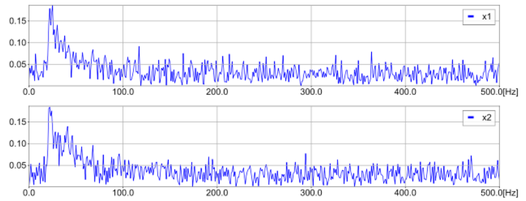

(b2) Fourier spectrum of (b1).

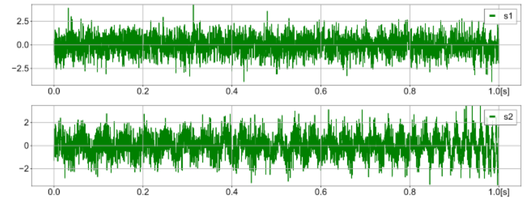

(b3) Output of ICA for (b1).

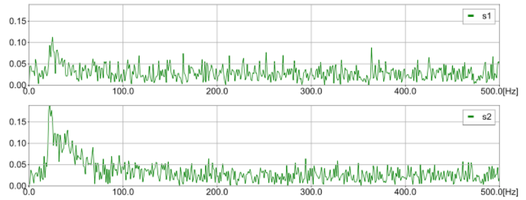

(b4) Fourier spectrum of (b3).

injection wave = 1.0 x noise

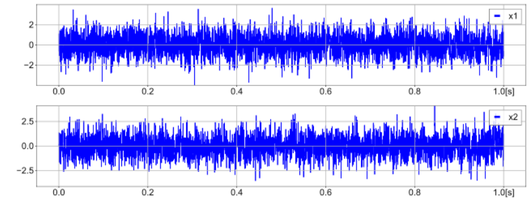

(c1) Input signals with $|h_{\mathrm{insp}}(t=1)|/\overline{|n_{\mathrm{G}}(t)|} = 1.0$.

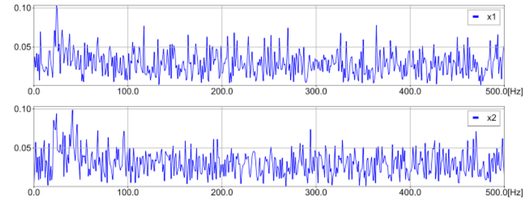

(c2) Fourier spectrum of (c1).

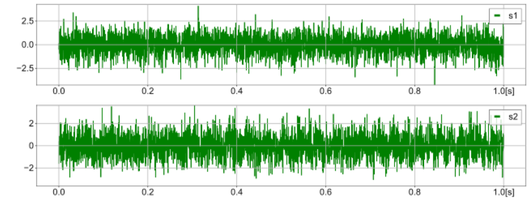

(c3) Output of ICA for (c1).

(c4) Fourier spectrum of (c3).

Test 2: Hanford/Livingston real noise data+sinusoidal-wave injection

$$\text{Model 2}: \begin{cases} x_1(t) = n_{\mathrm{H}}(t) + \sin(2\pi f t), \\ x_2(t) = n_{\mathrm{L}}(t) + \sin(2\pi f t) \end{cases}$$

Hanford/Livingston data around GW150914
f=213Hz sinusoidal-wave injection

→ can extract if SNR >10

SNR = 20

input x(t)

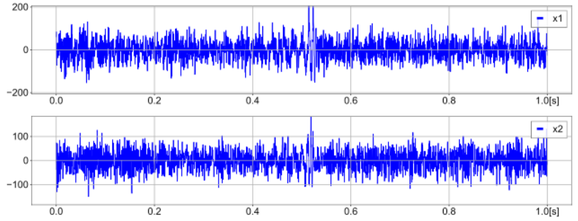

(a1) Input signals of SNR 20.

input x(f)

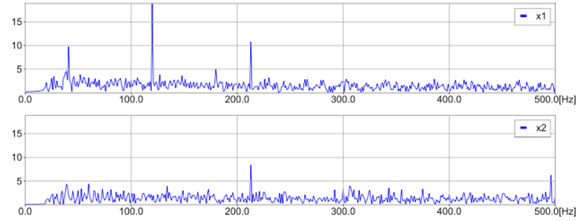

(a2) Fourier spectrum of (a1).

output s(t)

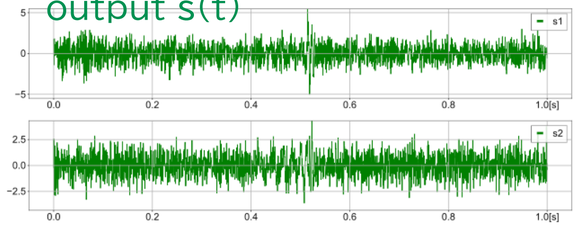

(a3) Output of ICA for (a1).

output s(f)

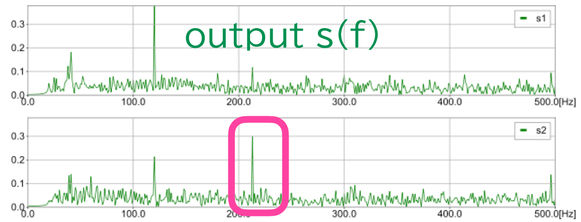

(a4) Fourier spectrum of (a3).

SNR = 10

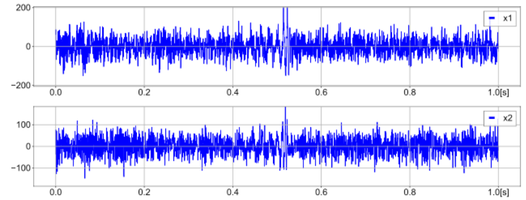

(b1) Input signals of SNR 10.

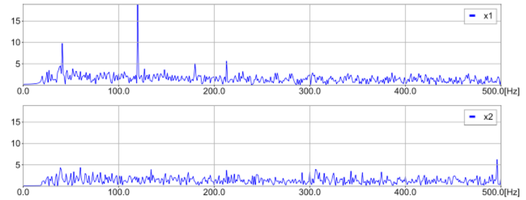

(b2) Fourier spectrum of (b1).

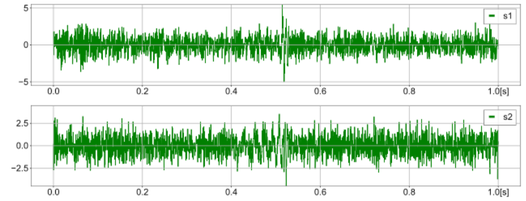

(b3) Output of ICA for (b1).

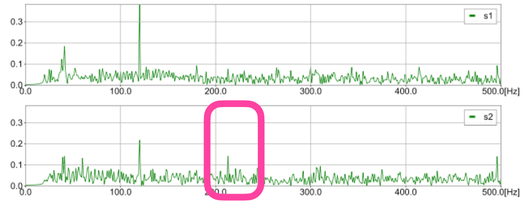

(b4) Fourier spectrum of (b3).

SNR = 5

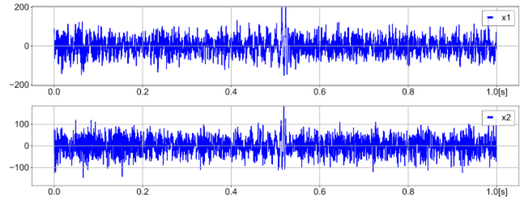

(c1) Input signals of SNR 5.

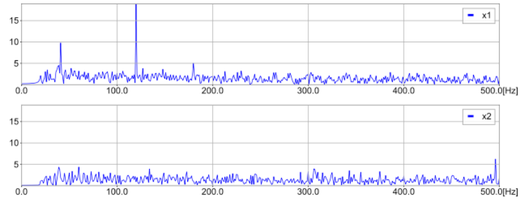

(c2) Fourier spectrum of (c1).

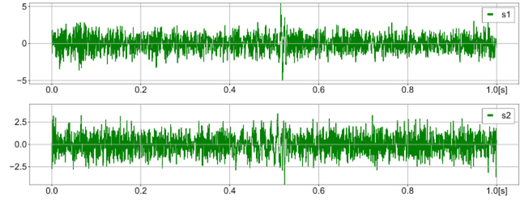

(c3) Output of ICA for (c1).

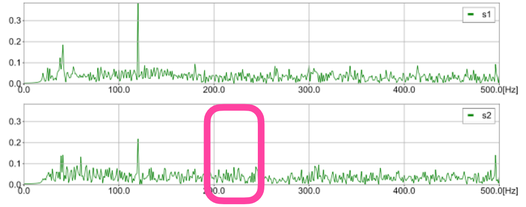

(c4) Fourier spectrum of (c3).

Test 3: Hanford/Livingston real noise data+inspiral-wave injection

$$\text{Model 3}: \begin{cases} s_1(t) = n_{\rm H}(t) + h_{\rm insp}(t; t_0, M_c), \\ s_2(t) = n_{\rm L}(t) + h_{\rm insp}(t; t_0, M_c). \end{cases}$$

Hanford/Livingston data around GW150914
inspiral-wave injection

➡ can recognize if SNR >15

SNR = 20.9

input x(t)

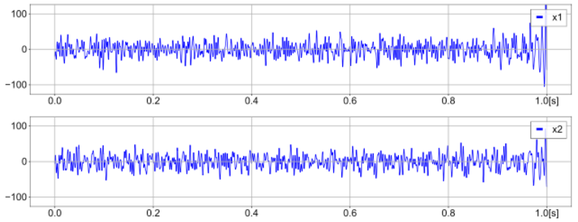

(a1) Input signals of SNR 20.9.

input x(f)

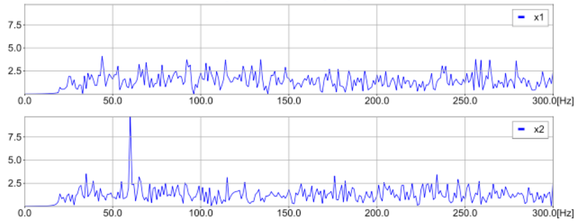

(a2) Fourier spectrum of (a1).

output s(t)

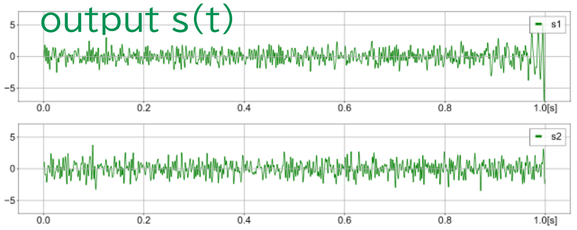

(a3) Output of ICA for (a1).

output s(f)

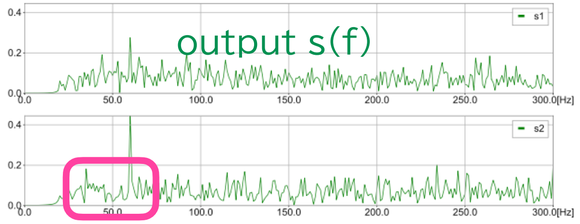

(a4) Fourier spectrum of (a3).

SNR = 16.8

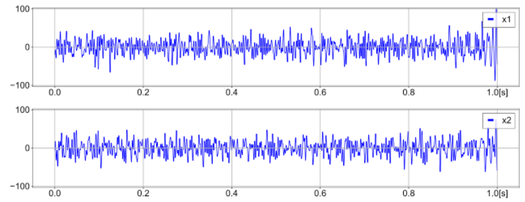

(b1) Input signals of SNR 16.8.

(b2) Fourier spectrum of (b1).

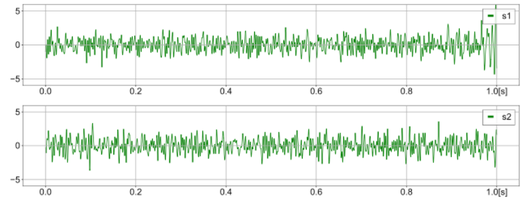

(b3) Output of ICA for (b1).

(b4) Fourier spectrum of (b3).

SNR = 10.5

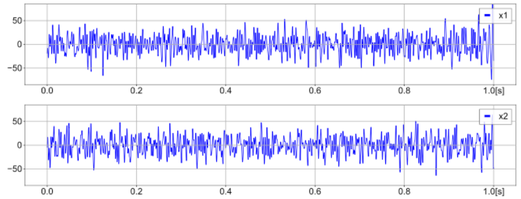

(c1) Input signals of SNR 10.5.

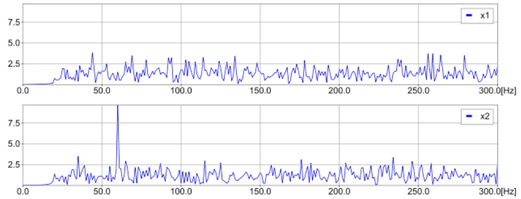

(c2) Fourier spectrum of (c1)

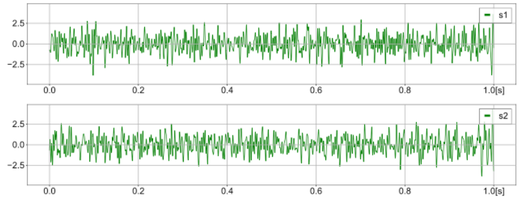

(c3) Output of ICA for (c1).

(c4) Fourier spectrum of (c3).

GW150914

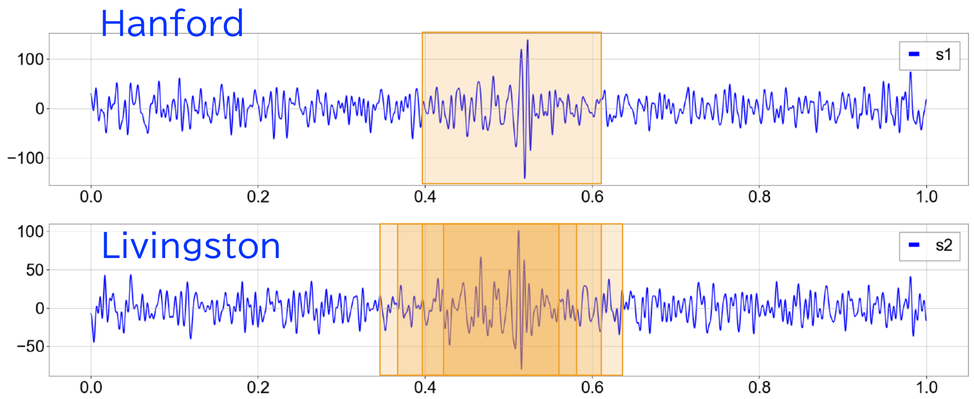

$$\mathcal{A} = \frac{A_1}{A_2}$$

$$A_a = \sum_{t=t_s}^{t_c} \tilde{\boldsymbol{s}}_a(t) \cdot \Delta t$$

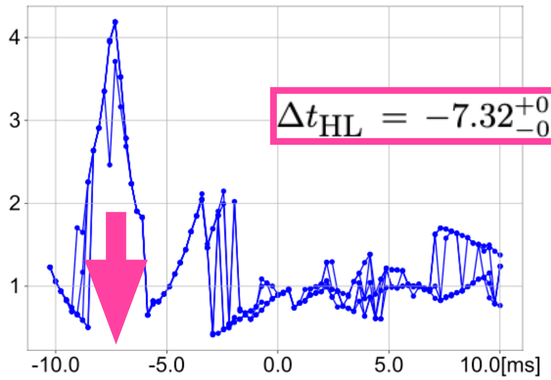

FIG. 5. The strength of the extracted signal, $\mathcal{A}$ [eq. (10)] as a function of $\Delta t_{\rm HL}$ for the case of GW150914. Five trials of different initial weight matrix are plotted at each $\Delta t_{\rm HL}$. We see the maximum is at $\Delta t_{\rm HL} = -7.32^{+0.15}_{-0.15}$ ms. Note that LIGO-Virgo paper [1] shows $\Delta t_{\rm HL} = 6.9^{+0.5}_{-0.4}$ ms.

LV paper says ▸ $\Delta t_{\rm HL} = -6.9^{+0.5}_{-0.4}$ ms.

$\Delta t_{\rm HL} = -7.32^{+0.15}_{-0.15}$ ms.

input x(t)

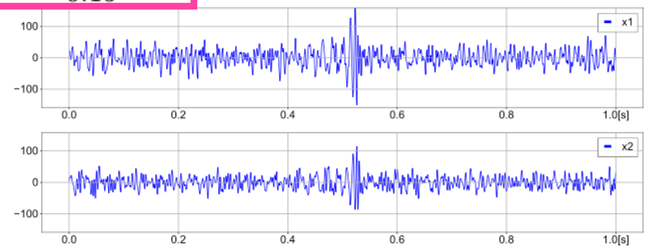

(a) Input signals with $\Delta t_{\rm HL} = -7.32$ ms. The data x1 and x2 are of Hanford and Livingston data, respectively.

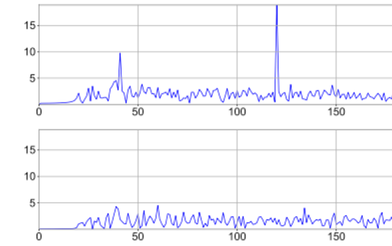

(b) Fourier spectrum of (a).

output s(t)

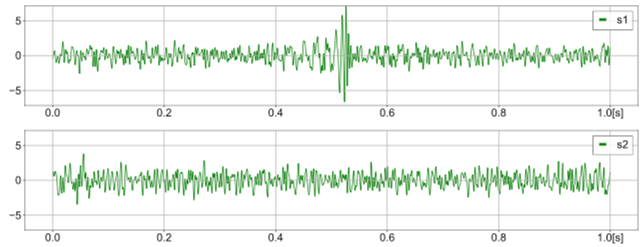

(c) Output of ICA.

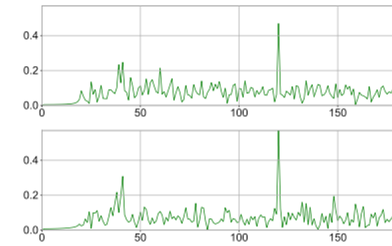

(d) Fourier spectrum of (c).

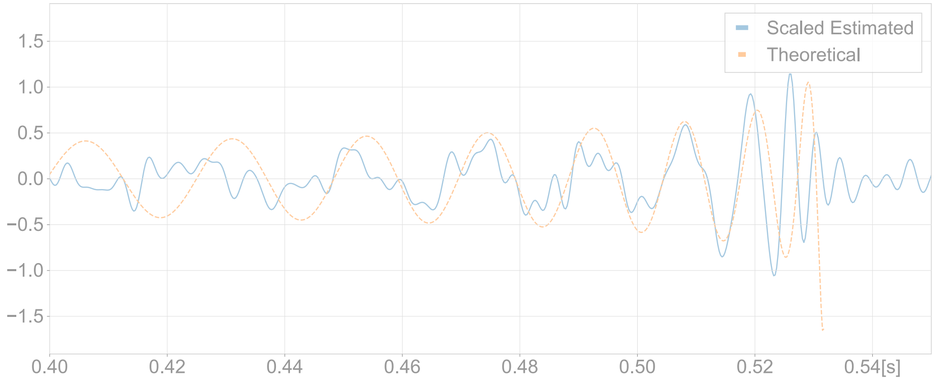

We derive Mc (obs) from the extracted GW by ICA

O1-O3 BBH events （high SNR 12 events + GW190521）

10

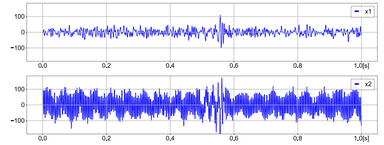

(a1) Input signals of GW190521_074359 with $\Delta t_{\rm HL} = -6.35$ ms. The data x1 and x2 are of Hanford and Livingston data, respectively.

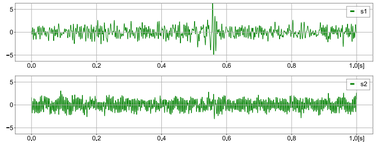

(a2) Output of ICA for GW190521_074359.

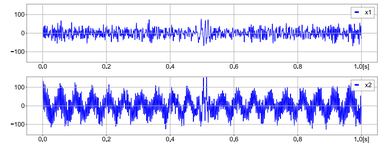

(b1) Input signals of GW191109_010717 with $\Delta t_{\rm HL} = +3.17$ ms. The data x1 and x2 are of Hanford and Livingston data, respectively.

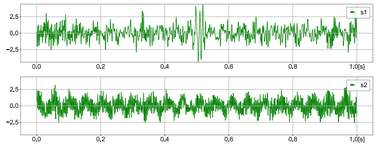

(b2) Output of ICA for GW191109_010717.

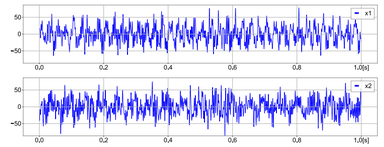

(c1) Input signals of GW191204_171526 with $\Delta t_{\rm HL} = -2.44$ ms. The data x1 and x2 are of Hanford and Livingston data, respectively.

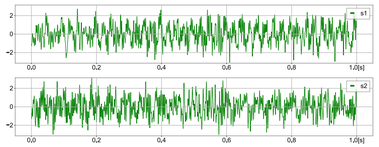

(c2) Output of ICA for GW191204_171526.

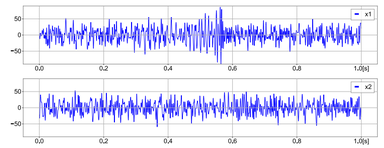

(d1) Input signals of GW191216_213338 with $\Delta t_{\rm HV} = -11.0$ ms. The data x1 and x2 are of Hanford and Virgo data, respectively.

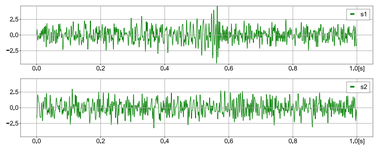

(d2) Output of ICA for GW191216_213338

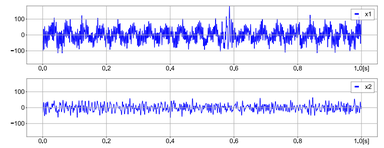

(e1) Input signals of GW200112_155838 with $\Delta t_{\rm LV} = -23.2$ ms. The data x1 and x2 are of Livingston and Virgo data, respectively.

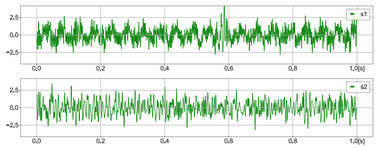

(e2) Output of ICA for GW200112_155838.

FIG. 7. Input and Output data of ICA analysis.

11

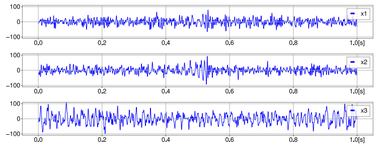

(f1) Input signals of GW170814 with $\Delta t_{\rm HL} = -8.06$ ms and $\Delta t_{\rm HV} = +0.98$ ms. The data x1, x2, and x3 are of Hanford, Livingston, and Virgo, respectively.

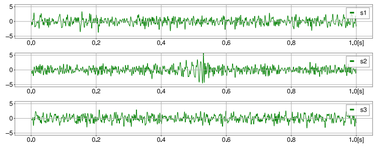

(f2) Output of ICA for GW170814.

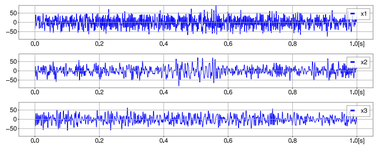

(g1) Input signals of GW190412 with $\Delta t_{\rm HL} = -3.91$ ms and $\Delta t_{\rm HV} = -13.92$ ms. The data x1, x2, and x3 are of Hanford, Livingston, and Virgo, respectively.

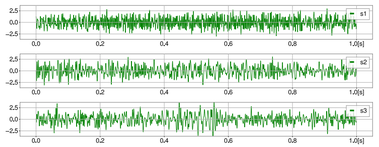

(g2) Output of ICA for GW190412.

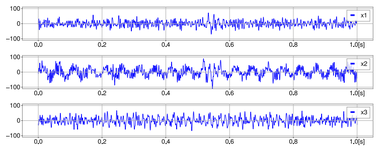

(h1) Input signals of GW190521 with $\Delta t_{\rm HL} = +2.93$ ms and $\Delta t_{\rm HV} = -25.15$ ms. The data x1, x2, and x3 are of Hanford, Livingston, and Virgo, respectively.

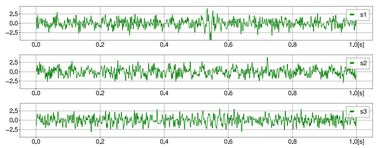

(h2) Output of ICA for GW190521.

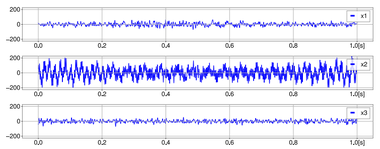

(i1) Input signals of GW190814 with $\Delta t_{\rm HL} = +2.20$ ms and $\Delta t_{\rm HV} = +21.24$ ms. The data x1, x2, and x3 are of Hanford, Livingston, and Virgo, respectively.

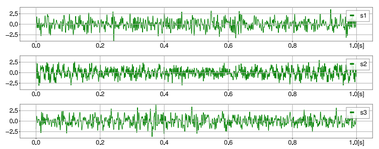

(i2) Output of ICA for GW190814.

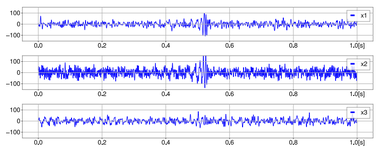

(j1) Input signals of GW200129_065458 with $\Delta t_{\rm HL} = +3.42$ ms and $\Delta t_{\rm HV} = -18.31$ ms. The data x1, x2, and x3 are of Hanford, Livingston, and Virgo, respectively.

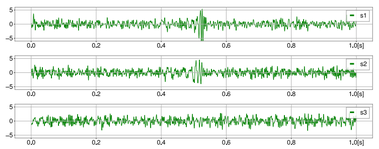

(j2) Output of ICA for GW200129_065458.

FIG. 7. Input and Output data of ICA analysis (cont.)

12

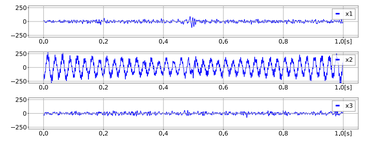

(k1) Input signals of GW200224_222234 with $\Delta t_{\rm HL} = -3.66$ ms and $\Delta t_{\rm HV} = -9.28$ ms. The data x1, x2, and x3 are of Hanford, Livingston, and Virgo, respectively.

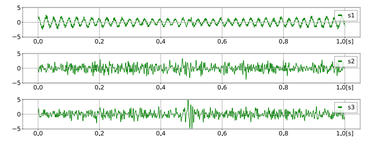

(k2) Output of ICA for GW200224_222234.

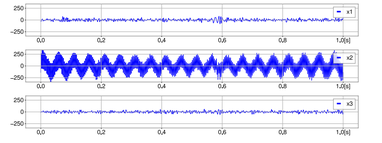

(l1) Input signals of GW200311_115853 with $\Delta t_{\rm HL} = -3.66$ ms and $\Delta t_{\rm HV} = -27.10$ ms. The data x1, x2, and x3 are of Hanford, Livingston, and Virgo, respectively.

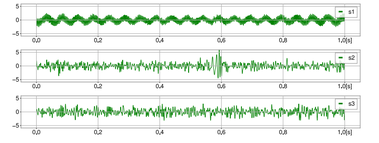

(l2) Output of ICA for GW200311_115853.

FIG. 7. Input and Output data of ICA analysis (cont.)

報告されたおもな重力波（2024 年 6 月現在）

連星の質量を M_1, M_2 としたときの，チャープ質量 $M_c = (M_1 M_2)^{3/5}/(M_1+M_2)^{1/5}$，質量比（中央値の比）$M_2/M_1$，有効スピン $\chi_{\rm eff}$，最終的に形成された BH の質量 $M_{\rm final}$(NS を含む場合は全質量 $M_{全} = M_1 + M_2$)，距離，波源特定精度（平方度）$(\Delta\theta)^2$，シグナル・ノイズ比 (SNR) を示す．幅のある量は 90% の信頼区間．(種類ごとに日付順．BBH については，GW190521 と SNR が 17.3 より大きいもののみ．)

イベント（BBH）	$M_c(M_\odot)$	質量比	$\chi_{\rm eff}$	$M_{\rm final}(M_\odot)$	距離 (Mpc)	$(\Delta\theta)^2$	SNR
GW150914	$28.6^{+1.7}_{-1.5}$	0.86	$-0.01^{+0.12}_{-0.13}$	$63.1^{+3.4}_{-3.0}$	440^{+150}_{-170}	250	26
GW170814	$24.1^{+1.4}_{-1.1}$	0.82	0.07			92	17.7
GW190412	$13.3^{+0.5}_{-0.5}$	0.32	0.21			240	19.8
GW190521	$63.3^{+19.6}_{-14.6}$	0.58	-0.14			000	14.3
GW190521_074359	$32.8^{+3.2}_{-2.8}$	0.77	0.1			470	25.9
GW190814	$6.11^{+0.06}_{-0.05}$	0.11	0			22	25.3
GW191109_010717	$47.5^{+9.6}_{-7.5}$	0.72	0.-29			600	17.3
GW191204_171526	$8.56^{+0.41}_{-0.28}$	0.72	0.16			350	17.4
GW191216_213338	$8.33^{+0.22}_{-0.19}$	0.64	0.11			490	18.6
GW200112_155838	$27.4^{+2.6}_{-2.1}$	0.79	0.06			300	19.8
GW200129_065458	$27.2^{+2.1}_{-2.3}$	0.84	0.11			130	26.8
GW200224_222234	$31.1^{+3.3}_{-2.7}$	0.82	0.1			50.0	20
GW200311_115853	$26.6^{+2.4}_{-2.0}$	0.81	-0.02			35	17.8

O1-O3 BBH events （high SNR 12 events + GW190521）

TABLE III. Results of the wave extractions by ICA for large SNR events in O1-O3. The column obs shows which detector (Hanford/Livingston/Virgo) observed. SNR is the network signal-to-noise ratio (centered value) which is announced in GWOSC (https://gwosc.org). $\Delta t_{\rm HL}$ is the time shift between Hanford data and Livingston data, $t_{\rm L} - t_{\rm H}$, in ms when ICA shows the best separation of the signal. $\mathcal{A}$ is the ratio of extracted signal to the other noise(s) evaluated by eq. (10). $\mathcal{R}$ is the residuals of the extracted waveform and estimated inspiral waveform, (11), between $[t_c - 0.15\ \text{ms}, t_c]$. See table IV for comparisons of chirp-mass and red-shift.

event	obs	SNR	$\Delta t_{\rm HL}$ (ms)	$\Delta t_{\rm HV}$ (ms)	$\Delta t_{\rm LV}$ (ms)	$\mathcal{A}$	$\mathcal{R}/10^{-12}$	ref.
GW150914	HL	26.0	$-7.32\pm^{1.5}_{1.5}$	–	–	4.19	5.88	Fig.4
GW190521_074359	HL	25.9	$-6.35\pm^{0.98}_{0.49}$	–	–	1.83	10.3	Fig.7(a)
GW191109_010717	HL	17.3	$3.17\pm^{0.98}_{0.73}$	–	–	3.40	18.4	Fig.7(b)
GW191204_171526	HL	17.5	$-2.44\pm^{0.49}_{0.73}$	–	–	2.07	3.27	Fig.7(c)
GW191216_213338	HV	18.6	–	$-11.0\pm^{1.5}_{0.73}$	–	3.08	2.09	Fig.7(d)
GW200112_155838	LV	19.8	–	–	$-23.2\pm^{0.49}_{0.24}$	2.43	10.5	Fig.7(e)
GW170814	HLV	17.7	$-8.06\pm^{0.49}_{0.98}$	$0.98\pm^{2.4}_{0.24}$	–	3.54	5.07	Fig.7(f)
GW190412	HLV	19.8	$-3.91\pm^{0.24}_{0.24}$	$-13.92\pm^{0.98}_{0.49}$	–	2.21	4.40	Fig.7(g)
GW190521	HLV	14.3	$2.93\pm^{0.49}_{1.2}$	$-25.15\pm^{0.49}_{1.7}$	–	2.85	31.8	Fig.7(h)
GW190814	HLV	25.3	$2.20\pm^{0.49}_{0.24}$	$21.24\pm^{0.73}_{0.24}$	–	2.00	1.65	Fig.7(i)
GW200129_065458	HLV	26.8	$3.42\pm^{0.98}_{0.24}$	$-18.31\pm^{0.24}_{0.24}$	–	3.96	11.3	Fig.7(j)
GW200224_222234	HLV	20.0	$-3.66\pm^{2.7}_{0.24}$	$-9.28\pm^{0.24}_{0.98}$	–	3.28	13.4	Fig.7(k)
GW200311_115853	HLV	17.8	$-3.66\pm^{0.73}_{1.2}$	$-27.10\pm^{2.2}_{2.2}$	–	3.17	4.34	Fig.7(l)

extracted GW strength vs noise
similar value to all

residuals of extracted GW minus
GW waveform model small for high SNR

O1-O3 BBH events （high SNR 12 events + GW190521）

TABLE IV. Comparisons of chirp mass, $M_c^{\rm source}$, shown in GWOSC and the one obtained by ICA,$M_c^{\rm obs}$ from the best fit inspiral-wave model. The difference can be regard as redshift factor $(1 + z_{\rm ICA})$. The redshift factor in GWOSC, z, is also shown.

			GWOSC		ICA		
event	obs	SNR	$M_c^{\rm source}/M_\odot$	z	$M_c^{\rm obs}/M_\odot$	$z_{\rm ICA}$	ref.
GW150914	HL	26.0	$28.6^{+1.7}_{-1.5}$	$0.09^{+0.03}_{-0.03}$	30.8	$0.077^{+0.06}_{-0.06}$	Fig.4
GW190521_074359	HL	25.9	$32.8^{+3.2}_{-2.8}$	$0.21^{+0.10}_{-0.10}$	36.4	$0.11^{+0.10}_{-0.10}$	Fig.7(a)
GW191109_010717	HL	17.3	$47.5^{+9.6}_{-7.5}$	$0.25^{+0.18}_{-0.12}$	53.7	$0.13^{+0.22}_{-0.19}$	Fig.7(b)
GW191204_171526	HL	17.5	$8.56^{+0.41}_{-0.28}$	$0.34^{+0.25}_{-0.18}$	11.1	$0.29^{+0.04}_{-0.06}$	Fig.7(c)
GW191216_213338	HV	18.6	$8.33^{+0.22}_{-0.19}$	$0.07^{+0.02}_{-0.03}$	9.00	$0.08^{+0.03}_{-0.03}$	Fig.7(d)
GW200112_155838	LV	19.8	$27.4^{+2.6}_{-2.1}$	$0.24^{+0.07}_{-0.08}$	32.7	$0.19^{+0.10}_{-0.10}$	Fig.7(e)
GW170814	HLV	17.7	$24.1^{+1.4}_{-1.1}$	$0.12^{+0.03}_{-0.04}$	26.0	$0.08^{+0.05}_{-0.06}$	Fig.7(f)
GW190412	HLV	19.8	$13.3^{+0.5}_{-0.5}$	$0.15^{+0.04}_{-0.04}$	14.8	$0.11^{+0.04}_{-0.04}$	Fig.7(g)
GW190521	HLV	14.3	$63.3^{+19.6}_{-14.6}$	$0.56^{+0.36}_{-0.27}$	81.7	$0.29^{+0.39}_{-0.30}$	Fig.7(h)
GW190814	HLV	25.3	$6.11^{+0.06}_{-0.05}$	$0.05^{+0.01}_{-0.01}$	6.35	$0.04^{+0.01}_{-0.01}$	Fig.7(i)
GW200129_065458	HLV	26.8	$27.2^{+2.1}_{-2.3}$	$0.18^{+0.05}_{-0.07}$	30.6	$0.13^{+0.10}_{-0.08}$	Fig.7(j)
GW200224_222234	HLV	20.0	$31.1^{+3.3}_{-2.7}$	$0.32^{+0.08}_{-0.11}$	37.6	$0.21^{+0.11}_{-0.12}$	Fig.7(k)
GW200311_115853	HLV	17.8	$26.6^{+2.4}_{-2.0}$	$0.23^{+0.05}_{-0.07}$	31.0	$0.17^{+0.09}_{-0.10}$	Fig.7(l)

We derive Mc (obs) from the extracted GW by ICA
Use LVK paper Mc (source) and derive (1+z) from our data
all z are consistent

Gravitational-wave Extraction using Independent Component Analysis

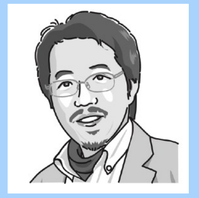

Hisaaki Shinkai, Rika Shimomura, Yuuichi Tabe
(Osaka Institute of Tech., Japan)

arXiv:2503.14179

- We proposed a new method for GW extraction.
- Injection tests show effectiveness for SNR>15 for real noise
- We applied the method for 12 real events.
  - can extract the waveform, consistent Mc(1+z) with GWTC3
    - GW waveforms are consistent for all events

- Laptop PC can handle
  (10 minutes for 2-detector data,
  a couple of hours for 3-detector data)

Advantages

More precise arrival time can be derived

- can apply more presice sky localization

No templates required

- Test of GR
- Unknown GW

Notes

- Coincident data is necessary.
- ICA decomposed waveform
  do not have information of amplitude,
  can be in the inverted phase.

This work was supported by JSPS KAKENHI Grants No. 24K07029 and 18K03630.